ELSEVIER

Journal of Power Sources 53 (1995) 63–74

JOURNAL OF POWER SOURCES

Influence of bismuth on the age-hardening and corrosion behaviour of low-antimony lead alloys in lead/acid battery systems

L.T. Lam [a,*], T.D. Huynh [a], N.P. Haigh [a], J.D. Douglas [a], D.A.J. Rand [a], C.S. Lakshmi [b], P.A. Hollingsworth [b], J.B. See [b], J. Manders [c], D.M. Rice [c]

[a] *CSIRO, Division of Mineral Products, PO Box 124, Port Melbourne, Vic. 3207, Australia*

[b] *Pasminco Research Centre, PO Box 175, Boolaroo, NSW 2284, Australia*

[c] *Pasminco Limited, PO Box 129K, Melbourne, Vic. 3001, Australia*

Received 21 September 1994; accepted 27 October 1994

Abstract

The effects of bismuth additions in the range 0.006–0.086 wt.% on the metallurgical and electrochemical properties of Pb–1.5 wt.% Sb alloy are investigated. The self-discharge behaviour of batteries produced with grids of the doped alloys is also evaluated. Addition of bismuth is found to exert no significant effects on the age-hardening behaviour, general microstructure or grain size of the alloy. It does, however, influence the morphology of the eutectic in the inter-dendritic regions. The latter changes from a mainly lamellar to an irregular type with increasing bismuth content. The corrosion rate of the grid decreases with increase of the bismuth content. Attack occurs preferentially in the inter-dendritic regions where there is an enrichment of both antimony and bismuth. Electron-probe microanalysis shows that the corrosion zone consists of a tri-layered structure, namely: a dense, continuous, inner layer ($PbO_{1.1}$); a central layer ($PbO_{1.8} \cdot PbSO_4$); a porous outer layer $n(PbO_{1.8}) \cdot PbSO_4$, with $n = 2$–8. In the latter, the value of n increases in the direction of corrosive penetration into the grid. Data from atomic absorption spectrometric analysis reveal that bismuth, after oxidative leaching from the grid substrate, is retained mainly in the corrosion layer. A key observation is that bismuth (i.e., up to ~0.09 wt.%) does not affect the self-discharge behaviour of batteries.

Keywords: Bismuth; Age-hardening; Corrosion; Lead–antimony alloys; Lead/acid batteries

1. Introduction

Bismuth is usually present in primary and secondary lead as an impurity. Consequently, the effect of residual bismuth on battery performance has been the subject of considerable concern. Although numerous investigations have been conducted, there is still extensive debate over whether bismuth is either beneficial or detrimental to the performance of lead/acid batteries. A recent review on the influence of bismuth has been presented by Koop et al. [1] and the data have been found to be both confusing and contradictory. Furthermore, most of the alloys that have been tested are lead–bismuth binary types that are not relevant to conventional battery systems.

The overall strategy of the Pasminco/CSIRO research programme is to determine the effect(s) of minor elements in lead materials on the performance of lead/acid batteries. The objectives include an examination of the role of bismuth. In a previous study [2], we have reported the influence of bismuth, added to the positive and negative active materials, on the performance of either flooded-electrolyte or valve-regulated lead/acid (VRLA) batteries. For automotive batteries, doping with bismuth produces no significant differences in JIS (Japan Industrial Standard) cycle life. By contrast, both the capacity and the endurance of VRLA batteries are found to be enhanced by the presence of bismuth.

Following on from this exploratory work, the research programme has been extended to assess the effects of incorporating bismuth in conventional, low-antimony and lead–calcium-based grid alloys. The investigation reported here is the first stage of this project and aims

* Corresponding author.

SSDI 0378-7753(94)02159-Z

to determine the effect(s) of bismuth, added to conventional, low-antimony alloy, on the age-hardening, microstructure and corrosion behaviour of the grid, as well as on the corresponding self-discharge performance of flooded-electrolyte automotive batteries.

2. Experimental

2.1. Grid casting

Low-antimony alloy grids, with different levels of bismuth addition, were cast using a Wirtz 40C grid caster. The grids were air-cooled after casting. The bulk compositions of the grids are given in Table 1. The grids have a nominal composition of 1.5 wt.% Sb (note, hereafter, the grid alloy will be denoted as Pb–1.5Sb). The variation in bismuth level had no significant effect on either the performance of the grid caster or the quality of the grids produced.

2.2. Hardness measurements

Periodic measurements of hardness were conducted over a period of ~90 days. This involved the use of a Matsuzawa DVK-2 hardness tester set in the Brinell mode. A ball of diameter = 1 mm was used as the indentor with a loading speed of 300 μm s^{-1} and a loading time of 5 s. A load of 1 kgf was applied.

The Brinell Hardness (HB) numbers were computed using the following formula [3]:

$$HB = 2P/\{3.1416D[D - \sqrt{(D^2 - d^2)}]\} \quad (1)$$

where, P = applied load (kgf), D = diameter of the ball (mm), and d = mean diameter of the impression (mm).

Hardness measurements were performed on samples that had been mounted in Struers Epofix cold mounts and ground with successively finer grades of SiC paper down to 4000 μm. The measurements were made at either the grid/wire intersection or the centre of the lug. For data obtained within the first 24 h of casting, however, the measurements were conducted on ground as-cast grids without mount. Although the cooling rates at the lug regions could vary slightly from those at the grid wires, no significant differences were observed. Indeed, the latter were found to be within the limits of experimental error. Therefore, for each measurement, three hardness values were taken (i.e., one reading at the lug centre and two at the grid/wire intersections). The average value was then used for plotting graphs of hardness versus ageing time.

Table 1
Composition (wt.%) of lead–antimony alloy grids

Pb–Sb alloy	Sb	Bi	As	Sn	Cu	Se
Alloy 1	1.45	0.006	0.20	0.163	0.04	0.02
Alloy 2	1.50	0.025	0.20	0.149	0.04	0.02
Alloy 3	1.40	0.053	0.21	0.159	0.04	0.02
Alloy 4	1.55	0.086	0.20	0.124	0.04	0.02

2.3. Microstructure

Metallographic samples were mounted using Struers Epofix cold mount at room temperature. The mounted samples were ground and polished with SiC papers down to 4000 μm. The following procedure was used to polish and etch the grid-alloy samples:

(i) chemical polishing by immersion for 1–2 min in a solution that contained 100 parts acetic acid and 10 parts (30%) hydrogen peroxide;

(ii) swabbing the darkened surface of the sample with concentrated nitric acid and rinsing with water;

(iii) chemical etching for 10–15 s by swabbing with a cotton bud dipped in 100 ml of a solution containing 10 g ammonium molybdate and 25 g citric acid;

(iv) rinsing with tap water and air drying at room temperature.

The microstructures of the samples were examined with either an Olympus PMG3 optical microscope or a Jeol JSM-252 III scanning electron microscope (SEM).

2.4. Corrosion tests

Corrosion tests were conducted on four 2 V cells that were connected in series. Each cell was assembled by placing five positive grids and six pasted negative plates in a rack that provided an inter-plate spacing of 5 mm. The bismuth content in the positive grids was the same within each cell, but different between cells. Sulfuric acid solution (1.275 sp. gr.) was introduced and the cells were maintained at 40 °C. A constant current of 0.5 A/grid was then applied for about two weeks. After a certain interval (i.e., 3–4 days), one positive grid, one negative plate and a small quantity of electrolyte (i.e., ~100 ml) were removed from each cell. The current was reduced by 0.5 A and the corrosion test continued. This process was repeated for all grids. After removal, each corroded grid was washed, dried and weighed. The corrosion layer was dissolved in a boiling 'mannitol' solution that had the composition shown in Table 2. Treatment for 5–20 min was required for complete removal of the corrosion layer. The amount of corrosion product was then determined either from the difference in the weight of the grid before and after digestion, or from the difference in the weight of the grid before the corrosion test and that after digestion. No significant difference was observed between these two procedures.

Table 2
Composition of chemical solution used to dissolve the corrosion layer

Sodium hydroxide (g)	100
Dihydrochloride hydrazine (g)	4
Mannitol (g)	20
Water (cm^3) [a]	1000
Operating temperature (°C)	100

[a] To make solution up to the volume given (i.e., 1000 cm^3).

Table 3
Paste formulae for positive and negative plates

Component	Positive plate	Negative plate
Leady oxide (kg)	3	3
Fibre (g)	1.5	1.8
Stearic acid (g)		1.8
$BaSO_4$ (g)		11.1
Vanisperse (g)		11.1
Carbon black (g)		6.3
1.40 sp. gr. H_2SO_4 (cm^3)	280	240
Water (cm^3)	400	380
Acid-to-oxide ratio (%)	6.5	5.6
Paste density (g cm^{-3})	4.2–4.3	4.3–4.4

The amounts of bismuth and antimony in both the 'mannitol' solution and the electrolyte, as well as on the negative plate, were also analyzed by atomic absorption spectrometry. A fresh grid was placed in another boiling 'mannitol' solution for the same period (i.e., 5–20 min). It was confirmed that no weight loss had occurred for the fresh grid before and after immersion in this solution. It was found, however, that small amounts of bismuth and antimony leached into the 'mannitol' solution. These values were used as the base-line for calculations of the concentrations of the two respective species in the corrosion layer. At the end of the corrosion test, two positive grids were collected. One grid was used for analysis of the corrosion product, and the other for SEM examination. It should be noted that the tests on the corrosion behaviour of low-antimony alloy grids with various bismuth contents were performed in duplicate.

2.5. *Self-discharge test*

Paste was made by combining a ball-mill oxide (bismuth-free), sulfuric acid, water, and additive (for negative plates only) in the proportions given in Table 3. The paste was then applied evenly, by hand, to lead–antimony grids that contained different bismuth contents (see Table 1). Plate curing was performed at 50 °C/high relative-humidity (r.h.) for 24 h, followed by drying for a further 24 h. The dried plates were then assembled into NS40 type, 2 V cells that comprised four positives (enclosed in Daramic separator envelopes) and five negatives. The positive and negative grids in each cell contained the same level of bismuth.

Sulfuric acid solution (1.07 sp. gr.) was introduced into each cell and the plates were allowed to stand in this solution for 30 min at 25 °C. Formation was undertaken with a constant current of 5 A for 20 h. After formation, the cell solution was replaced with 1.30 sp. gr. acid and a constant current of 2.5 A was applied until the terminal voltage and acid density exhibited no appreciable change (i.e., within 3%) between three, consecutive, hourly readings. This condition was taken as the initial fully-charged state of the cell. The acid density was then adjusted to lie between 1.270 and 1.275 g cm^{-3}. Two, successive, *C*/5 discharge capacities were determined in order to check the stability of the cell capacity. The cells were then fully charged (i.e., charge-to-discharge ratio = 1.2) and allowed to stand at open circuit at 25 °C for 30 days. After this period, the *C*/5 capacities of the cells were evaluated. Any decrease in capacity will be due to the self-discharge of the cell during open-circuit standing.

3. Results

3.1. *Age-hardening and metallographic structure of grid alloys*

Age-hardening of grid alloys is an important parameter for the successful manufacture of lead/acid batteries. It allows plates to be machine-handled during paste mixing and reduces the reject rate of plates. Fig. 1 presents the age-hardening behaviour of air-cooled, lead–antimony grid alloys with various bismuth levels. The results reveal clearly that bismuth additions of up to 0.09 wt.% have no significant effect on either the hardening rate or the hardness values of the grids. For all the alloys, the hardness value increases from 9 to ~17 HB during ~60 days following casting.

The microstructures of air-cooled, lead–antimony alloy grids with various bismuth contents are shown in Fig. 2. The optical micrographs reveal that during solidification, the growth of lead in Pb–Sb grids gives rise to 'fir-tree' crystal structures; these are dendrites. The dendrites are built up with rounded crystal structures. There are no marked changes in either the microstructure or the grain size on increasing the level of bismuth to ~0.09 wt.%. Lead solid-solution dendrites are the first to freeze when liquid lead–antimony is cooled. As the lead dendrites grow into the lead–antimony liquid, the latter becomes rich in antimony until a composition of 13 wt.% is reached. The liquid (i.e., eutectic) surrounding the lead crystals then begins to freeze. Consequently, this gives rise to an antimony-rich phase in between the arms of the lead dendrites.

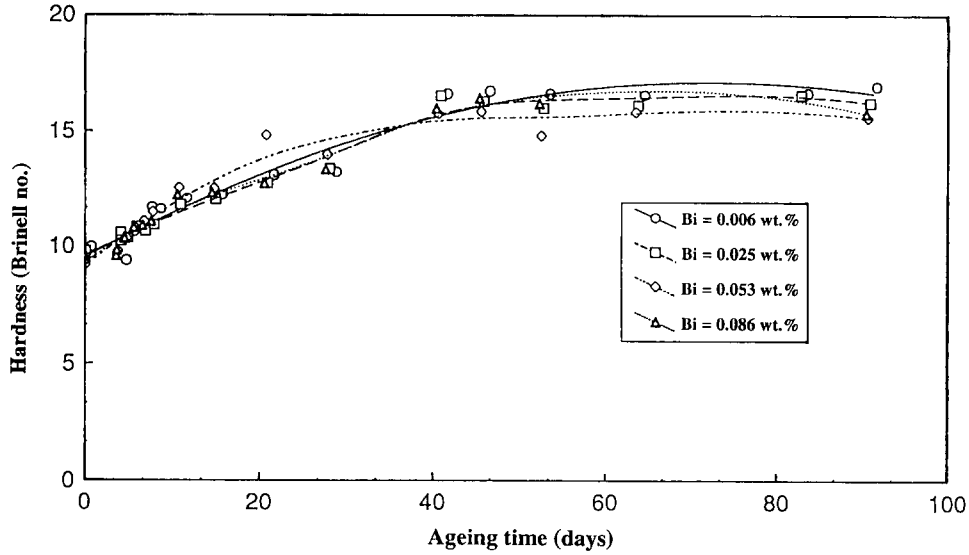

Fig. 1. Age-hardening behaviour of air-cooled Pb–1.5Sb alloy grids with given bismuth contents.

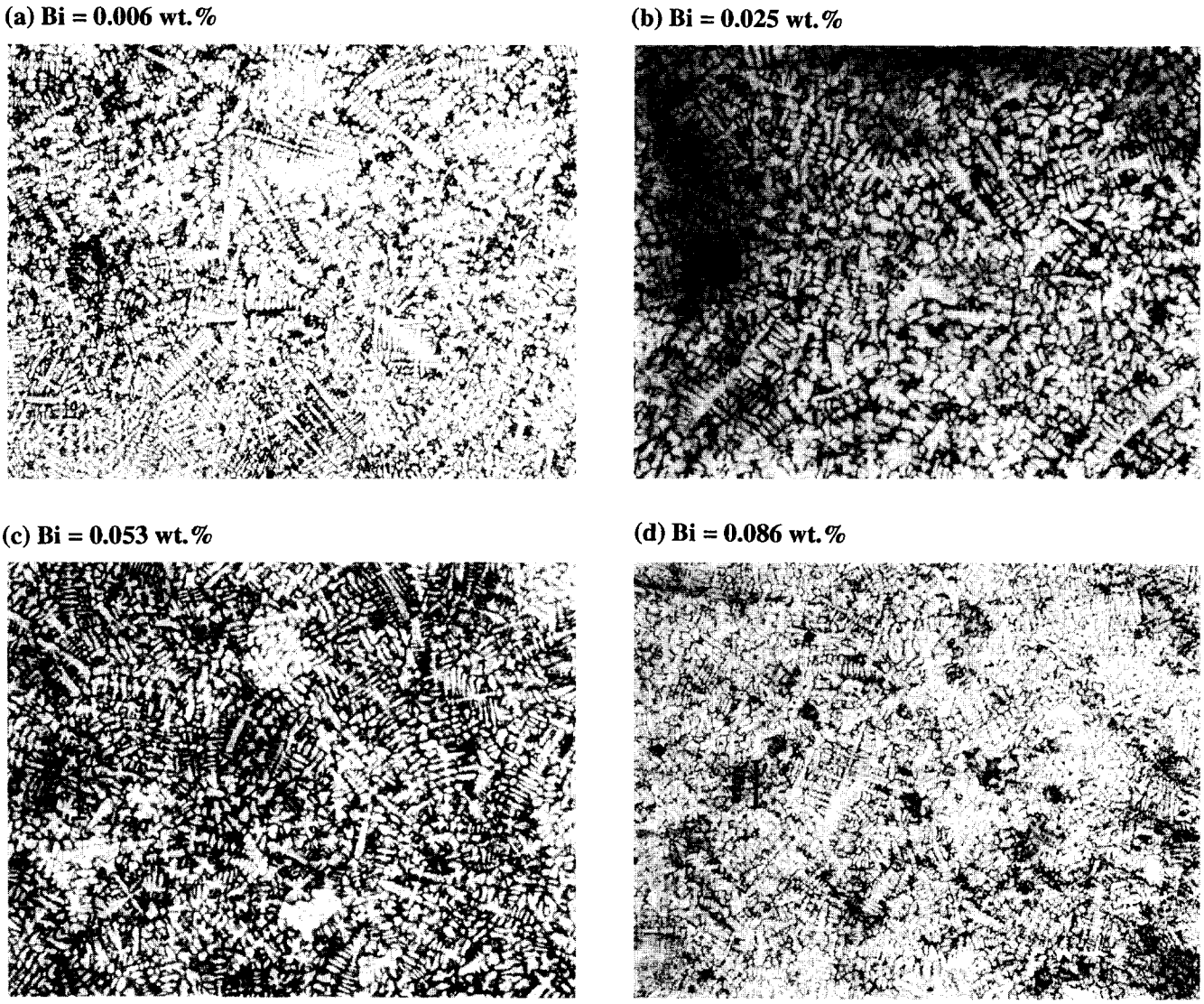

Fig. 2. Optical micrographs showing the microstructure of Pb–1.5Sb grids with given bismuth contents. Magnification bar: 100 μm.

The microstructures of the eutectic phase at the lead inter-dendrites are shown at high magnification in Fig. 3. At low bismuth levels, the antimony-rich phase consists mainly of a fine, lamellar, eutectic structure (Fig. 3(a)). This structure tends to become more irregular when the bismuth concentration is increased (Fig. 3(b)–(d)).

In summary, the addition of bismuth to Pb–1.5Sb alloy does not affect the age-hardening behaviour, general microstructure or grain size of the resulting grids. By contrast, the eutectic morphology changes slightly from a mainly lamellar structure to a more irregular structure with increasing bismuth content.

3.2. Grid corrosion

The corrosion behaviour of Pb–1.5Sb grids with various bismuth contents is represented by the weight loss versus time graph given in Fig. 4. During the first 7.1 days, the corrosion proceeds at almost the same rate for all the alloys, irrespective of the bismuth content. The reaction during this period represents the corrosive attack of the grids during plate formation, as well as during the early stages of cycling. With further treatment, the corrosion starts to slow down as the grids become covered with an appreciable thickness of corrosion material. The reaction simulates grid corrosion during battery service. At this stage, the rate of corrosion decreases with an increasing level of bismuth.

Fig. 5 shows the effect of bismuth content on the corrosion rate. The latter is presented as the average value of two trials. The data show that the corrosion rate decreases significantly from ~7.2 to ~4 mg per g of grid per day when the bismuth content in the grid is increased to ~0.09 wt.%. This indicates clearly that

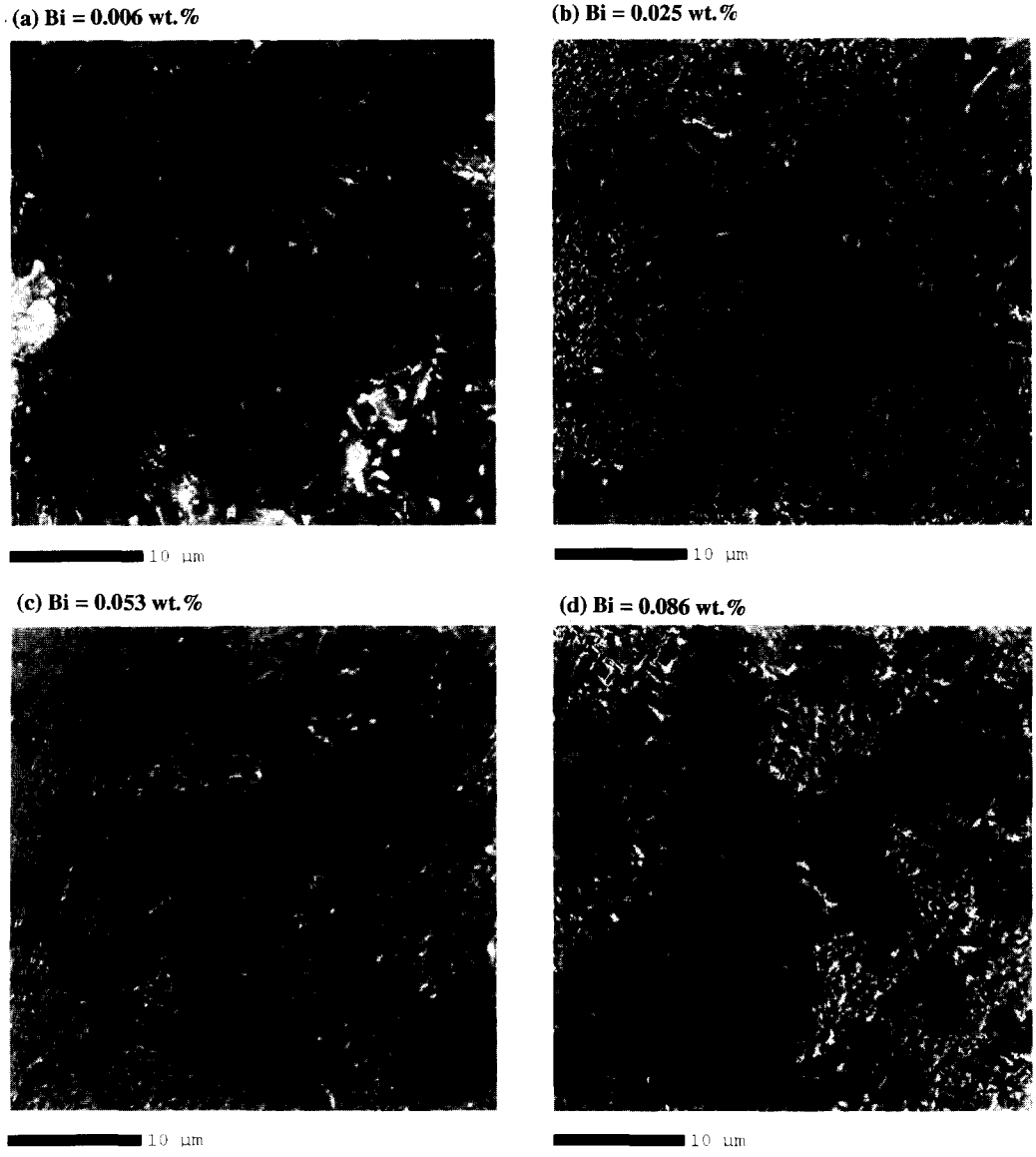

Fig. 3. Electron micrographs showing the effect of bismuth on the morphology of the eutectic phase. Magnification bar: 10 μm.

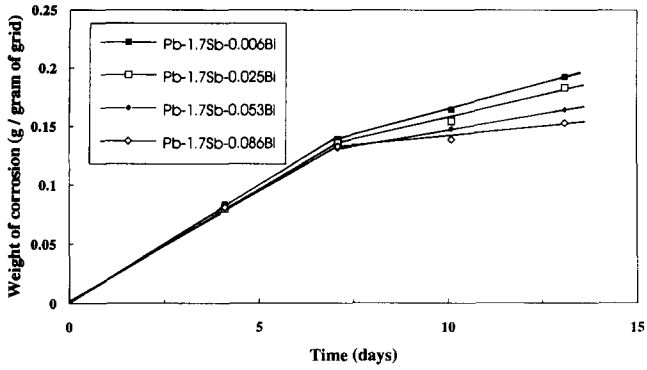

Fig. 4. Effect of bismuth on the corrosion (i.e., weight loss) of Pb–1.5Sb grids.

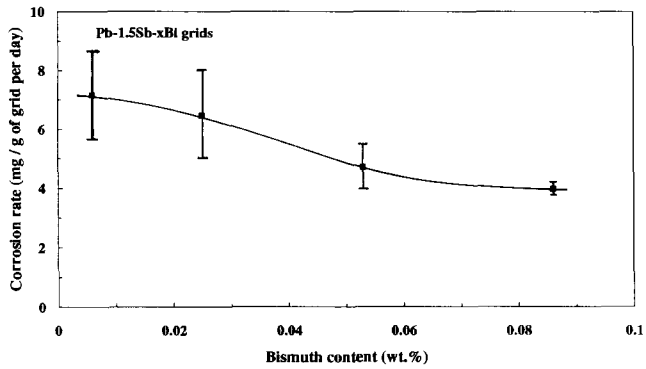

Fig. 5. Corrosion rate of Pb–1.5Sb grids as a function of bismuth content.

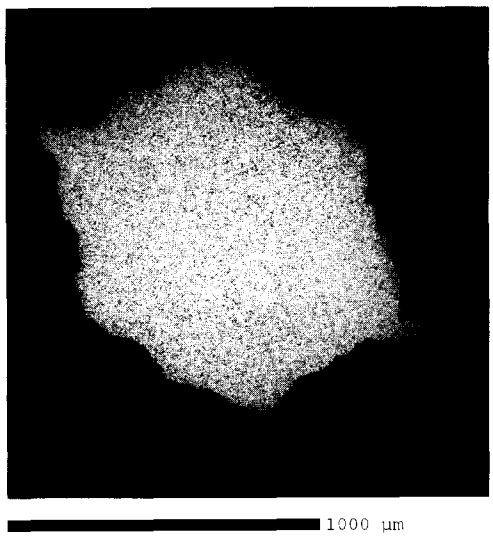

Fig. 6. Electron micrograph of the cross section of a grid wire (0.006 wt.% bismuth) before corrosion test. Magnification bar: 1000 μm.

the addition of bismuth (up to a level of 0.09 wt.%) to low-antimony alloy can suppress grid corrosion.

The corrosion layer was subjected to detailed analysis. A cross-sectional view of a grid prior to corrosion testing is presented in Fig. 6. The grid wire has an approximate oval-shaped cross section with a rough surface and two sharp ends in the direction of the long diameter. When a similar cross section is observed on a sample after ~13.1 days of corrosion (Fig. 7), it is seen that the corrosion layer becomes slightly thinner as the bismuth content is increased. Furthermore, the lead at the two sharp ends of the oval-shaped grid is undermined and, possibly, some incompletely oxidized lead particles become detached from the grid.

It is also found that the corrosion occurs preferentially at the inter-dendritic regions and grain boundaries, irrespective of the bismuth concentration (Fig. 8). The extent of this preferential attack, however, appears to be less when the bismuth content is increased. At certain locations, incompletely oxidized lead particles are left in the corrosion layer. These particles will be removed when the corrosion products are dissolved in 'mannitol' solution.

At higher magnification, electron micrographs (Fig. 9) of grids with 0.006 or 0.086 wt.% bismuth reveal that there are, in fact, three distinct corrosion zones: (i) a dense, continuous, inner layer; (ii) a porous, outer layer; (iii) another dense layer residing between the inner and outer layers. A similar multi-layered structure of corrosion products on low-antimony grids has been reported by Chen et al. [4]. Moreover, this structure resembles that observed [5,6] for pure-lead and lead–calcium grids. Electron microprobe analysis showed the inner layer adjacent to the lead dendrite to be composed of $PbO_{1.1}$. By contrast, the outer layer has a composition of $n(PbO_x)\cdot PbSO_4$, with $x=1.7$–1.9 and $n=2$–8. The value of n varies from location to location, but generally increases with penetration depth into the grid. The dense central layer between the outer and inner corrosion layers is a mixture of $PbO_{1.8}$ and $PbSO_4$ with a formula of $PbO_{1.8}\cdot PbSO_4$. Similar observations are also made for other alloys containing 0.025 or 0.053 wt.% bismuth.

3.3. Oxidative leaching of antimony and bismuth

The oxidative leaching that occurred during corrosion was monitored by atomic absorption spectrometry. The elements analyzed were antimony and bismuth in the positive-grid corrosion layer, the electrolyte, and the negative active material. The leaching of bismuth and antimony into the corrosion products at various intervals of time is presented in Fig. 10. For the same grid composition, the overall trend reveals that the level of each element in the corrosion layer increases with increasing exposure time, except for bismuth leaching from the grid containing 0.053 wt.% bismuth. In this grid, the concentration of bismuth in the corrosion layer decreases during the first 7.1 days, and then remains virtually unchanged thereafter.

The increase in concentration of antimony in the corrosion layer proceeds rapidly when the bismuth content in the grid is less than 0.053 wt.%. This increase,

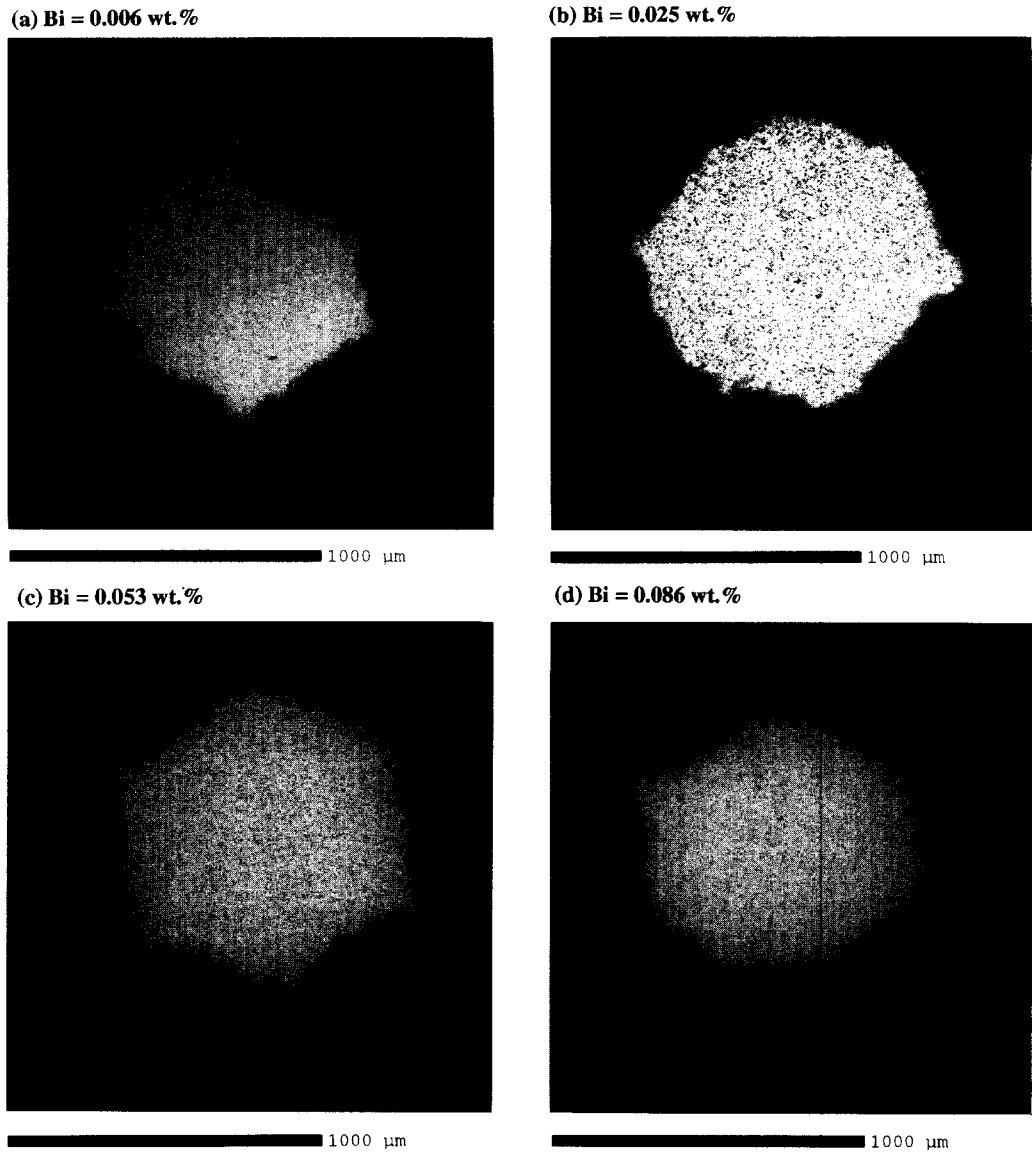

Fig. 7. Electron micrographs of the cross sections of corroded Pb–1.5Sb grids with given bismuth contents. Magnification bar: 1000 μm.

however, slows down when the bismuth content is equal to, or greater than, 0.053 wt.%. By contrast, the concentration of bismuth builds up steadily for grids containing bismuth below 0.053 wt.% and increases much faster for a grid with 0.086 wt.% bismuth. It is found that the weight percent of antimony or bismuth in the corrosion layer, under certain testing conditions, is greater than the corresponding value in the grid alloy (cf., Table 1).

Fig. 11 shows the concentrations of bismuth and antimony in the electrolyte following oxidative leaching from the grids. The results clearly suggest that there is little difference in bismuth dissolution from the various alloys; the level is very low, namely, less than ~1 ppm. By contrast, the concentration of antimony in the electrolyte is much higher (i.e., 4–12 ppm). For all the grids, the concentration of antimony passes through a minimum at an intermediate corrosion time of 7.1 days. There is however, an increase in antimony concentration with further exposure (to 13.1 days) for grids with bismuth up to 0.053 wt.%. By contrast, the level of antimony is virtually the same when the bismuth content is increased to 0.086 wt.%.

During the oxidation of all types of grids, no bismuth could be detected on the negative plates. The amount of antimony deposited on the negative plates shows almost the same trend as that found in solution. That is, an increase (from 0.028–0.033 to 0.049–0.053 wt.%) with increase in corrosion time (Fig. 12), except for the grid with a bismuth content of 0.086 wt.%. In the latter case, the deposition of antimony becomes almost constant after oxidation periods of greater than ~10.1 days.

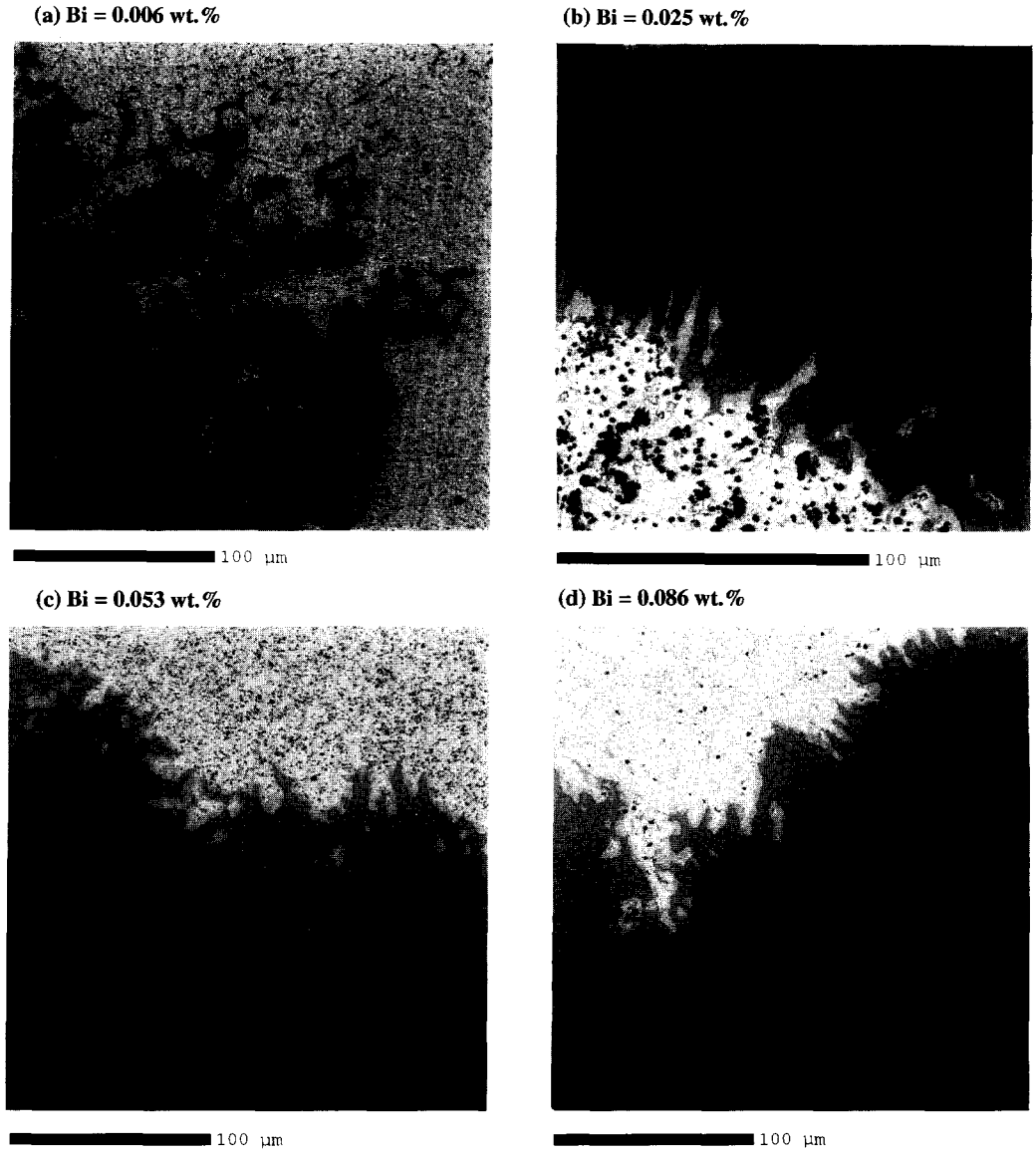

Fig. 8. Electron micrographs showing the penetration corrosion of Pb–1.5Sb grids with given bismuth contents. Magnification bar: 100 μm.

3.4. Self-discharge behaviour

Experimental studies show that the percentage of capacity retained by the cells after an open-circuit stand of one month was unaltered by the bismuth content in the grids. All cells yielded ~94% capacity (Fig. 13). This indicates that addition of bismuth to low-antimony, positive and negative grids does not affect the self-discharge behaviour of batteries.

4. Discussion

4.1. Effect(s) of bismuth on age-hardening of low-antimony lead alloys

Lead–antimony alloys have been the traditional choice of grid metal for lead/acid batteries. The industry has used alloys containing 1–11 wt.% Sb. The equilibrium diagram of this alloy system shows the presence of an eutectic phase that contains 13 wt.% Sb at 247 °C [7]. The maximum solubility of antimony in lead solid-solution is 2.5 wt.% at this eutectic temperature, but only 0.1 wt.% at room temperature. Since the solubility of antimony is extremely low at room temperature, there will be precipitation of finely-dispersed antimony within the lead–antimony solid-solution grains, both soon after casting and during ageing. This causes a gradual increase in the grid hardness (i.e., age-hardening).

On the other hand, the lead–bismuth binary phase diagram [8] indicates that bismuth forms a solid-solution with lead up to 18 wt.% bismuth at room temperature. At 184 °C, the bismuth solubility rises to 23.5 wt.%. The concentration of antimony in the grids employed in this study (i.e., 1.5 wt.%) is about 16 times greater

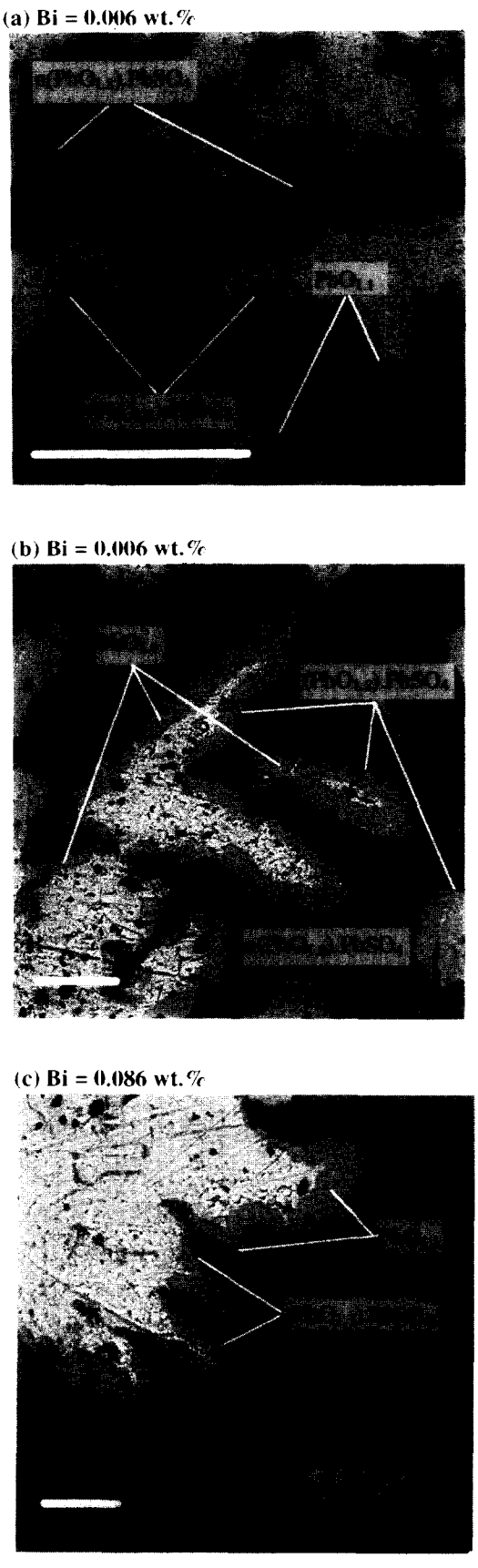

Fig. 9. Electron micrographs showing different phases (zones) of corrosion products developed on Pb–1.5Sb grids with given bismuth contents. Magnification bar: (a) 50 μm; (b), (c) 10 μm.

than the maximum level of bismuth (i.e., 0.086 wt.%). Consequently, the age-hardening of the grid should be dominated by the presence of antimony rather than by bismuth. In other words, the addition of bismuth to lead–antimony grids in amounts up to 0.086 wt.% has no significant effect on the age-hardening, overall microstructure or grain size of the resulting grids. It should be pointed out, however, that although bismuth can form a solid-solution with lead up to 18 wt.% Bi, the micro-segregation of bismuth at lead inter-dendrites and grain boundaries can also occur under rapid cooling during grid casting. The extent of this segregation process will increase with increase in the bismuth level. Thus, the regions at the lead inter-dendrites and grain boundaries will be enriched with both antimony and bismuth. This phenomenon can be seen from the antimony and bismuth maps that show the distribution of these two species in the grid (Fig. 14). The incorporation of bismuth into the lead inter-dendrites and grain boundaries may, in turn, modify the morphology of the eutectic (i.e., antimony-rich phase) from a lamellar to an irregular structure, as seen in Fig. 3.

4.2. Effect(s) of bismuth on corrosion behaviour of Pb–Sb alloys

The degree of structural homogeneity of an alloy will influence its corrosion behaviour. A homogeneous structure will favour a uniform attack throughout the entire metal surface, i.e., general corrosion. By contrast, a heterogeneous structure will promote selective attack only at some regions of the metal surface; this results in penetration corrosion. The presence of different phases in a metallic material exposed to the action of an anodic current may cause the more reactive phases to undergo a heavy attack, while the more inert zones remain practically intact. For the Pb–1.5Sb grid alloy used in this work, the preferential attack will take place at the lead inter-dendrites and grain boundaries where there is enrichment of both antimony and bismuth. This is because the two elements are more reactive than the surrounding lead during oxidation in sulfuric acid solution. In other words, antimony and bismuth will supply routes for penetration corrosion. This phenomenon is revealed clearly by scanning electron micrographs of the corroded grids (see Figs. 7 and 8).

Feliu et al. [9,10] have shown that the rate of the localized attack varies with both the form (i.e., lamellar or spherical shapes) and size of the second phase (i.e., Sb, Sn, Ag, etc.). The effect is more severe when the second phase consists of an almost continuous lamellar network, than when this phase is distributed in a discontinuous particulate form. This fact has already been pointed out by Mao et al. [11] in an attempt to explain the higher corrosion-resistance of certain lead alloys. Studies of the microstructure of lead–antimony

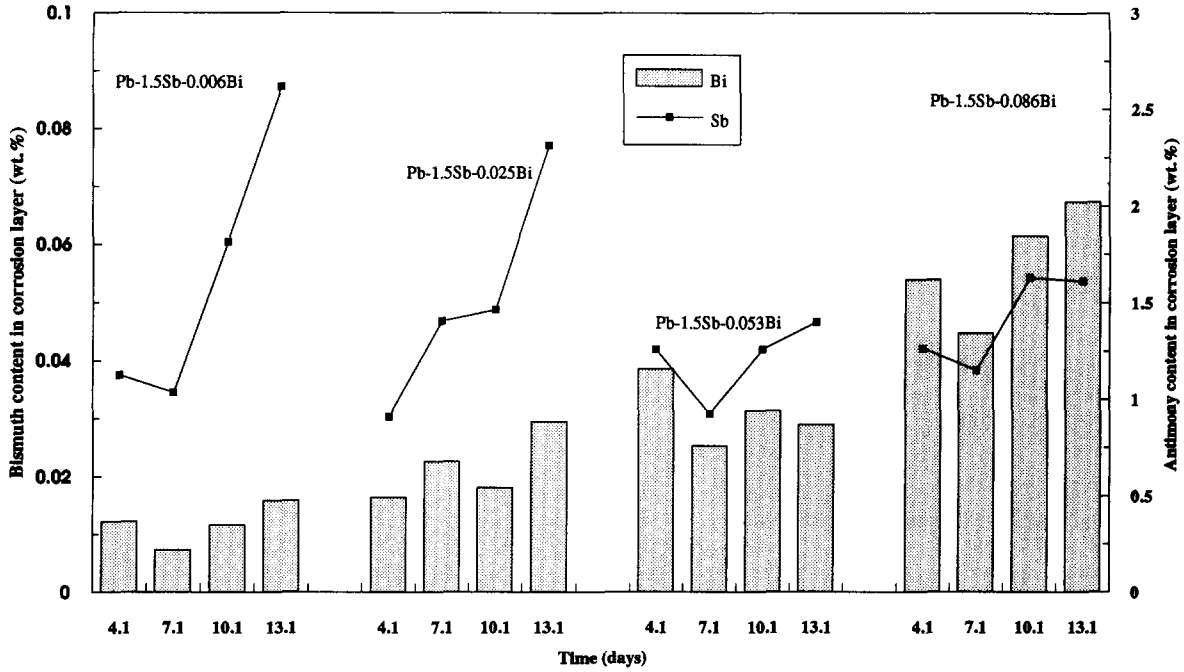

Fig. 10. Progressive change in concentration of antimony and bismuth ions in the corrosion layer during oxidative leaching of Pb–1.5Sb grids with given bismuth contents (sulfuric acid solution at 40 °C).

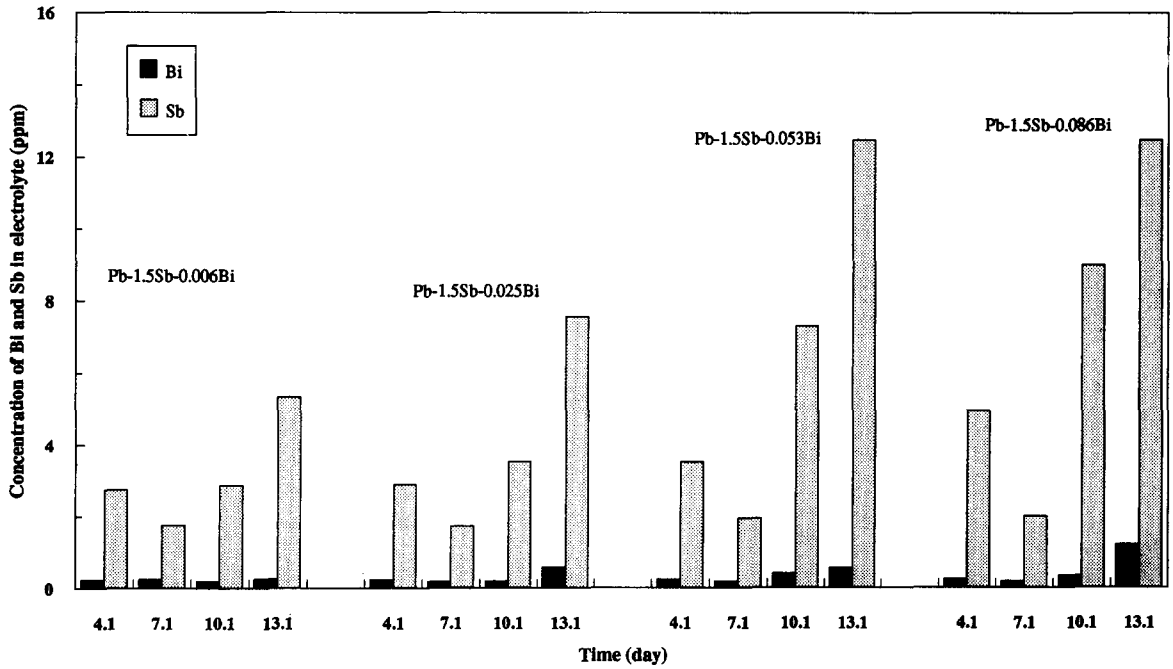

Fig. 11. Progressive change in concentration of antimony and bismuth ions in the electrolyte during oxidative leaching of Pb–1.5Sb grids with given bismuth contents (sulfuric acid solution at 40 °C).

alloys reveal that the addition of bismuth exerts no significant effect on either the structure or the size of the grains in the resulting grids (see Fig. 2), but does influence the morphology of the eutectic. The micro-segregation prefers to take the form of individual particles rather than a mixture of acicular and particulate shapes when the bismuth level is increased (Fig. 3). Thus, the degree of penetrative attack will be less when the grid contains high bismuth. This is confirmed by electron micrographs of corroded grids with different bismuth contents (Fig. 7). Furthermore, the advance of the penetrative attack may give rise to undermining and removal of particles from the lead-dendrite matrix (see Figs. 7–9). In this case, the weight losses determined by the removal of the corrosion product would also include the effect of this disintegration. With increase

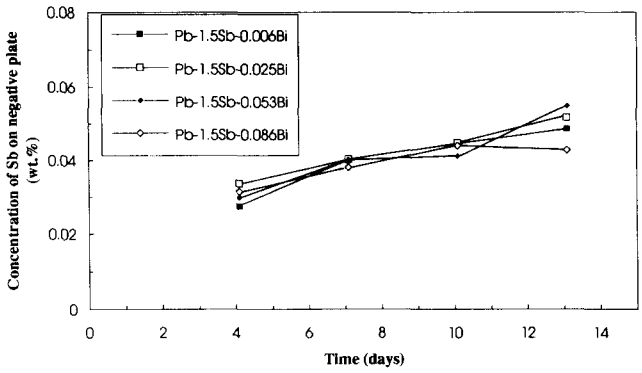

Fig. 12. Progressive change in concentration of antimony deposited on the negative plates during oxidative leaching of Pb–1.5Sb grids with given bismuth contents (sulfuric acid solution 40 °C).

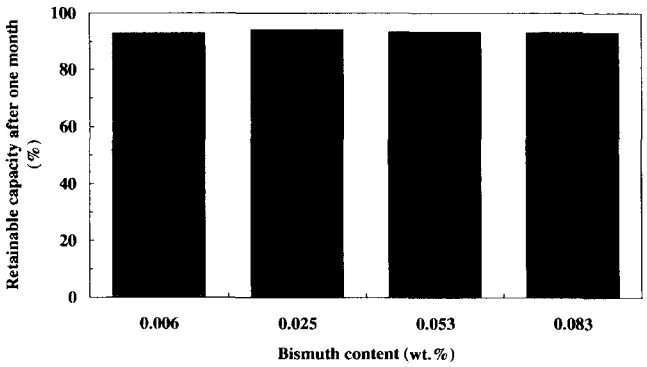

Fig. 13. Effect of bismuth content in the grid on the self-discharge behaviour of batteries.

of bismuth content, the penetrative attack becomes less and, consequently, the likelihood of undermining and breakdown of lead particles is correspondingly reduced. Therefore, the corrosion rate decreases with increase in the addition of bismuth.

As mentioned above, the concentration of both antimony and bismuth at the lead inter-dendrites and grain boundaries is much higher than in the bulk of the alloy (Table 1). Preferential attack at these regions will, of course, release appreciable amounts of these two elements into the thin corrosion layer. Thus, the weight percent of either antimony or bismuth in the corrosion product can be higher than that in the grid, as determined by the degree of penetration (see Fig. 10). Since the bulk concentration of antimony in the grids used in this research work is already low (i.e., ~1.5 wt.%) and a large amount is leached out during oxidation, the corrosion at the dendrites will approach that of pure lead or lead–calcium alloys [6,7]. The corrosion products give rise to a multi-layered structure.

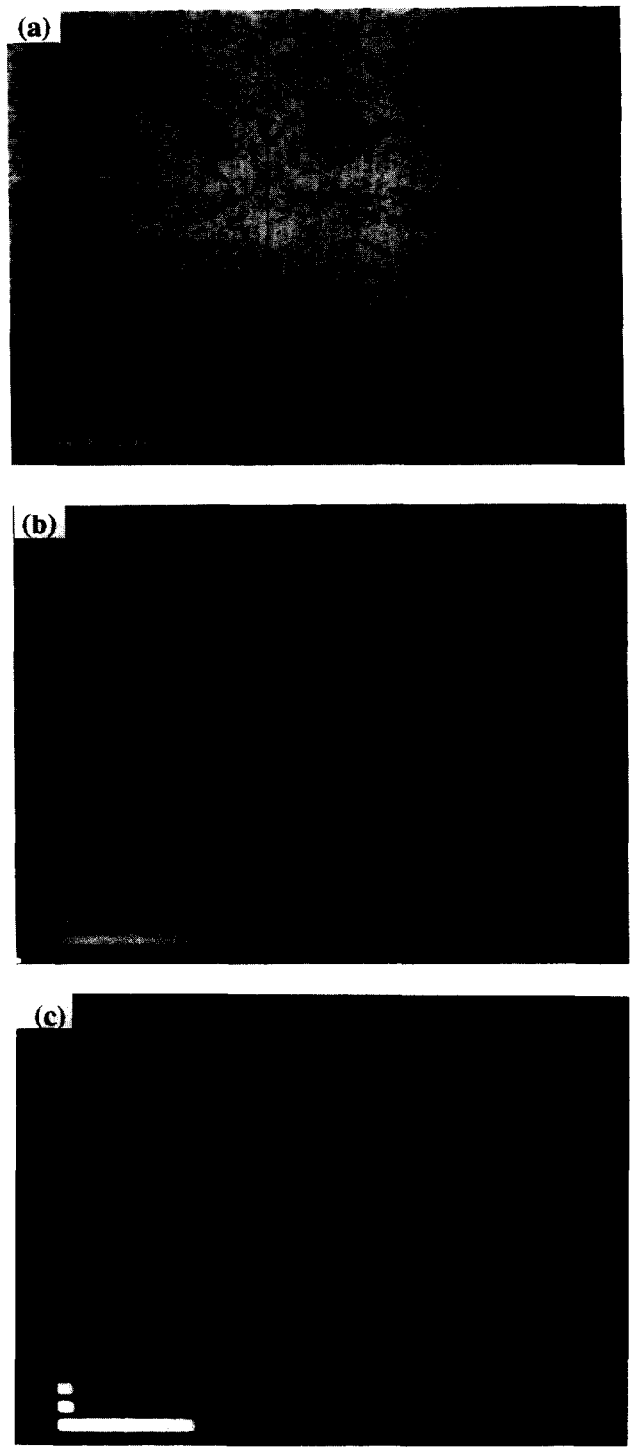

Fig. 14. Electron micrograph of (a) cross section of Pb–1.5Sb–0.086Bi grid and corresponding element maps showing: (b) distribution of antimony; (c) distribution of bismuth. Magnification bar: 100 μm.

5. Conclusions

The objective of this research programme has been to determine the changes in metallurgical and electrochemical properties of low-antimony grids (i.e., Pb–1.5Sb) when alloyed with various levels of bismuth. From the above experimental observations, the following conclusions can be drawn.

(i) The age-hardening, general microstructure and grain size of the grids are not affected by bismuth

additions up to ~0.09 wt.%. The morphology of the eutectic, however, tends to change from a lamellar structure towards a more irregular form when the bismuth content is increased.

(ii) The corrosion of bare grids in sulfuric acid is of the general type. Preferential attack takes place at the inter-dendritic regions and grain boundaries and the advance of this corrosion gives rise to undermining and detachment of lead particles from the dendrite matrix. This phenomenon is, however, less prominent when the bismuth level in the grid is increased. Consequently, the corrosion rate decreases with increasing bismuth content.

(iii) The corrosion products developed on low-antimony grids give rise to a tri-layered structure, namely: a dense, continuous, inner layer with a composition approaching that of 'PbO'; a porous outer layer having the formula $n(PbO_{1.8}) \cdot PbSO_4$ with $n = 2$–8; a third, central, layer with a composition of $PbO_{1.8} \cdot PbSO_4$.

(iv) Bismuth ions, after oxidative leaching from the grids, are retained mainly in the corrosion layer.

(v) The addition of bismuth up to ~0.09 wt.% has no major effects on the self-discharge behaviour of batteries.

References

[1] M.J. Koop, D.A.J. Rand and B. Culpin, *J. Power Sources, 45* (1993) 365.
[2] L.T. Lam, R. De Marco, J.D. Douglas, R. Pillig, D.A.J. Rand and J. Manders, *J. Power Sources, 48* (1994) 113.
[3] *Annual Book of ASTM Standards, Metals Test Method and Analytical Procedures,* Vol. 03.01, ASTM, Philadelphia, PA, 1985, p. 189.
[4] Z.W. Chen, J.B. See and W.F. Gillian, *J. Power Sources, 50* (1994) 47.
[5] K.R. Bullock and M.A. Butler, *J. Electrochem. Soc., 133* (1986) 1085.
[6] L.T. Lam, H. Ozgun, O. Lim, J.A. Hamilton, L.H. Vu, D.G. Vella and D.A.J. Rand, *J. Power Sources, 53* (1995) 215.
[7] G.W. Vinal, *Storage Batteries,* Willey, New York, 1955, p. 18.
[8] W. Hofmann, *Lead and Lead Alloys,* Springer, Berlin, 1970, pp. 40–44.
[9] S. Feliu and M. Morcillo, *Electrochim. Acta, 21* (1976) 1035.
[10] S. Feliu, E. Otero and J.A. Gonzalez, *J. Power Sources, 3* (1978) 145.
[11] G.W. Mao, J.G. Larson and P. Rao, *J. Inst. Met., 97* (1969) 343.